World Academy of Science, Engineering and Technology
International Journal of Geological and Environmental Engineering
Vol:18, No:4, 2024

# Petrology Investigation of Apatite Minerals in the Esfordi Mine, Yazd, Iran

Haleh Rezaei Zanjirabadi, Fatemeh Saberi, Bahman Rahimzadeh, Fariborz Masoudi, Mohammad Rahgosha



***Abstract*—**In this study, apatite minerals from the iron-phosphate deposit of Yazd have been investigated within the microcontinent zone of Iran in the Zagros structural zone. The geological units in the Esfordi area belong to the pre-Cambrian to lower-Cambrian age, consisting of a succession of carbonate rocks (dolomite), shale, tuff, sandstone, and volcanic rocks. In addition to the mentioned sedimentary and volcanic rocks, the granitoid mass of Bahabad, which is the largest intrusive mass in the region, has intruded into the eastern part of this series and has caused its metamorphism and alteration. After collecting the available data, various samples of Esfordi's apatite were prepared, and their mineralogy and crystallography were investigated using laboratory methods such as petrographic microscopy, Raman spectroscopy, EDS (Energy Dispersive Spectroscopy), and Scanning Electron Microscopy (SEM). In non-destructive Raman spectroscopy, the molecular structure of apatite minerals was revealed in four distinct spectral ranges. Initially, the spectra of phosphate and aluminum bonds with O2HO, OH, were observed, followed by the identification of Cl, OH, Al, Na, Ca and hydroxyl units depending on the type of apatite mineral family. In SEM analysis, based on various shapes and different phases of apatites, their constituent major elements were identified through EDS, indicating that the samples from the Esfordi mining area exhibit a dense and coherent texture with smooth surfaces. Based on the elemental analysis results by EDS, the apatites in the Esfordi area are classified into the calcic apatite group.

***Keywords*—**Petrology, apatite, Esfordi, EDS, SEM, Scanning Electron Microscopy, Raman spectroscopy.

## I. Introduction

MINERALOGY plays a vital role in understanding and elucidating various geological processes, providing us with valuable resources found within the Earth. In this regard, apatite, as one of the important minerals with its unique chemical composition and physical properties, plays an unparalleled role. Also, numerous studies have been conducted in this field, such as [1] and [2] which examine the Esfordi deposit, identifying the source of ore-forming fluids as evaporative brines and, in the second stage, fluids sourced from granitic intrusions. The study of [3] considers iron mineralization in the Bafq region to be associated with the early Cambrian granite genesis. This is because the iron-apatite mineralization in the Choghart mine with the Loko granite of the Zarigan is logically consistent in terms of age overlap. The evolution of melanephelinite melts in a rift environment is recognized by [12]. While others attribute their formation to carbonate magmatism in a rift environment [4]-[7]. Previous studies have shown [3], [12], [4], [7] that apatites occur in various regions worldwide and in different environments. Analyses have also indicated that the chemical compositions and crystalline properties of apatites are diverse. This information is crucial for understanding the origin and formation of apatites, as well as for the exploitation of resources. In this research, we have focused on investigating the specific characteristics of apatites, including mineralogy, crystallography, and gemology. This research utilized laboratory petrographic methods, Raman spectroscopy, and elemental analysis using EDS and SEM to investigate the apatites of the Esfordi region.

## II. Location of Case Study

The studied area is located in Yazd province and is recognized as one of the largest regions with iron deposits in the country. Experts in mineralogy and geology consider this area as one of the important mineral resources. In the Yazd region, the geological units belong to the pre-Cambrian to lower-Cambrian series, comprising a succession of carbonate rocks, shale, tuff, sandstone, and volcanic rocks. Additionally, the Bahabad granitoid massif is also situated in this area, which has had a significant influence on the geological history of the region (Fig. 1).

## III. Methodology

Initially, a final visit to the area was conducted for the purpose of controlling and revising the maps, as well as sampling apatite veins. After sampling, 15 thin section and two polished thin sections were prepared for petrological, mineralogical, mineral fabric in the laboratory of Shahid Beheshti University. Three apatite samples (SF-1, SF-2, SF-3) were separated for EDS analysis to identify the elemental composition of apatite, and SEM analysis was conducted to investigate the surface morphology and crystal structure of apatite crystals. Additionally, three samples (SF-11, SF-12, SF-13) were prepared for Raman study at Shahid Beheshti University, which will be discussed further below (Fig. 2).

## IV. Result and Discussion

### *A. Microscopic Studies of Apatites in the Esfordi Region*

In this section, we will examine the microscopic images of the studied apatite samples. In these studies, mineralogical

Haleh Rezaei Zanjirabadi is Student of Master, Shahid Beheshti University, Tehran, Iran.

Fatemeh Saberi is Ph.D Student, Department of Geology & Geological Engineering, University of North Dakota, ND, USA (e-mail: fatemeh.saberi@ndus.edu).

Bahman Rahimzadeh, Fariborz Masoudi, and Mohammad Rahgosha are with Faculty of Earth Science, Shahid Beheshti University, Tehran, Iran.

relationships were well investigated and studied. Briefly, it can be described that we have observed two generations of apatite in the Esfordi region, and based on observations, the second generation of apatites has succeeded the first-generation apatites (Fig. 3). Additionally, in some cases, we observed co-growth between apatites and calcite in the Esfordi mine, indicating a common origin of the fluid during the formation of these two minerals (Fig. 3).

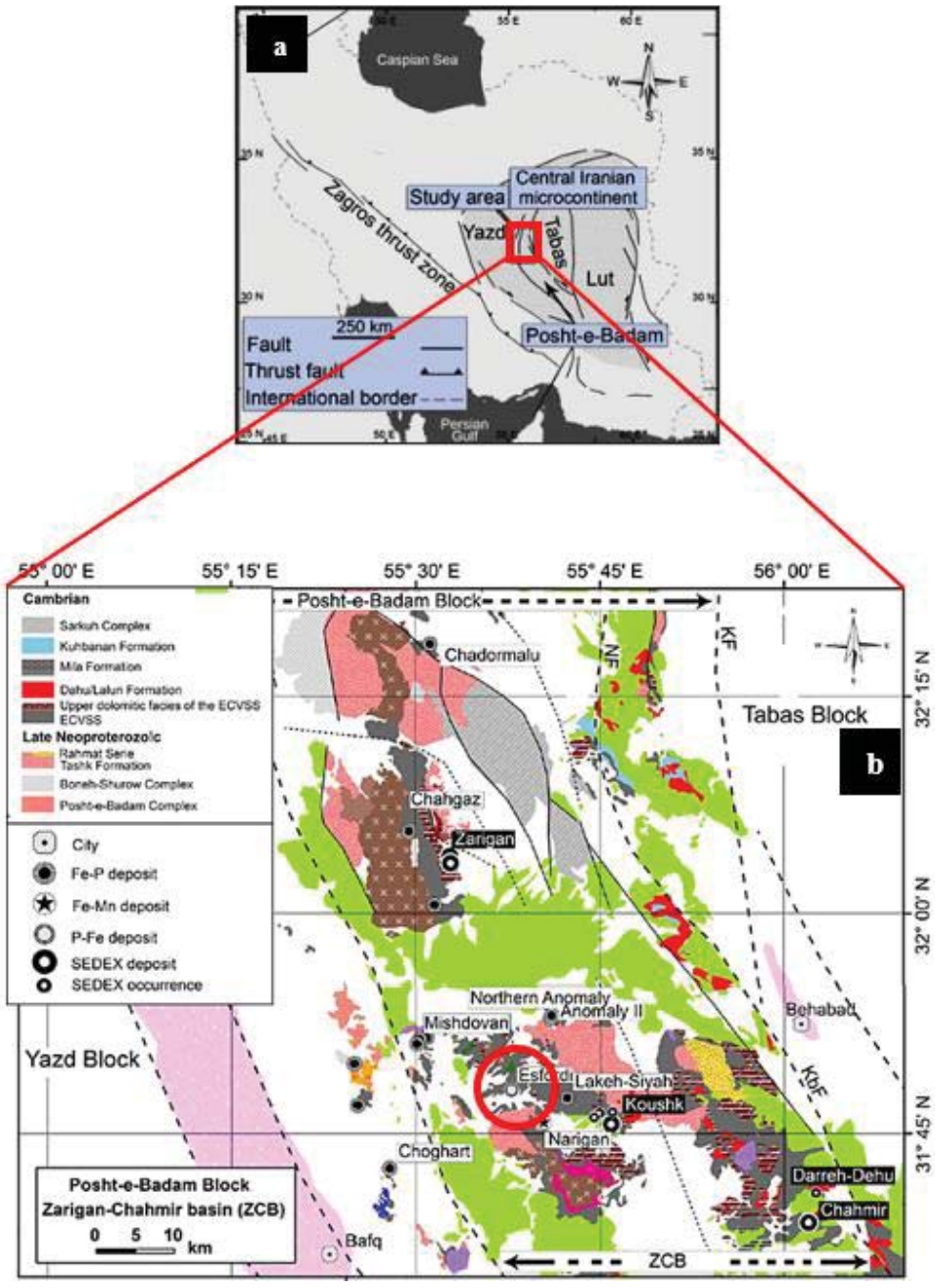


Fig. 1 (a) The location of the Esfordi region on the structural zone map (adapted from [13]) (b) Geological map of the Esfordi region and other adjacent deposits [8]

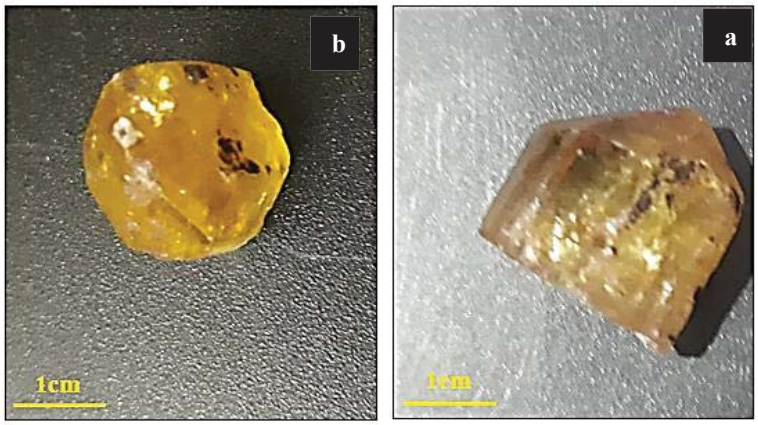


Fig. 2 (a) Representation of studied coarse-grained apatites from the Esfordi (Sf); (a), (b) Samples SF-1 and SF-2 selected from the phosphorus-iron mine in Esfordi, characterized by coarse-grained, yellow-colored crystals

*B. Raman Spectroscopy*

1. Raman Spectroscopy of Sf11 Sample from the Iron-Phosphate Mine of Esfordi

Based on the conducted Raman spectroscopy studies on the Sf11 sample (Fig. 4), the Raman spectroscopy of the sample in the 800-200 $cm^{-1}$ region indicates the presence of a crystalline lattice of O-P-O and O-Ca-O bands. In the 800-1600 $cm^{-1}$ region, the spectra can be divided into two sections. The first section is limited to the band range of 800 to 1200 $cm^{-1}$ and includes P-(O, OH, $H_2O$) and Ca-(O, OH, $H_2O$), while the second section, i.e., the range of 1600 to 1500 $cm^{-1}$, comprises phosphate units and Ca-O. In the region of 2000-2700 $cm^{-1}$, the spectrum of apatite and chlorapatite is associated with units within their structure. For example, these can include phosphate units, water units, calcium units, and hydroxyl chloro-fluoride units. Each of these units can exhibit different vibrations in the analyzed bands in Raman analysis. The region of 3500-3200 $cm^{-1}$ is associated with the presence of OH and chlorine in the mineral of interest, which is well observed in the Raman peaks of the sample [9]-[11].

2. Raman Spectroscopy of Sf12 Sample from the Iron-Phosphate Mine of Esfordi

Based on the conducted Raman spectroscopy studies on the SFF-12 sample (Fig. 5), the Raman spectroscopy of the sample in the 600-100 $cm^{-1}$ region indicates the presence of a crystalline lattice of O-P-O and O-Ca-O bands. In the area of 900-1600 $cm^{-1}$, there are minerals consisting of P-(O, OH, $H_2O$) and Ca-(O, OH, $H_2O$). In the region of 1800-2700 $cm^{-1}$, the spectrum of apatite and chlorapatite is associated with units within their structure. For example, these can include phosphate units, water units, calcium units, and hydroxyl chloro-fluoride units. Each of these units can exhibit different vibrations in the analyzed bands in Raman analysis. In the spectral range of 2900-3450 $cm^{-1}$, the presence of OH, (OH)-, and F units is observed [9]-[11].

3. Raman Spectroscopy of SF-13 Sample from the Iron-Phosphate Mine of Esfordi

Based on the conducted Raman spectroscopy studies on the SF-13 sample (Fig. 6), the Raman spectroscopy of the sample in the 1500-950 $cm^{-1}$ region indicates the presence of a crystalline lattice of O-P-O and O-Ca-O bands. In the 1200-1800 $cm^{-1}$ region, the spectra can be divided into two sections. The first section is limited to the band range of 1800 to 2250 $cm^{-1}$ and includes P-(O, OH, $H_2O$) and Ca-(O, OH, $H_2O$), while the second section, i.e., the range of 2600 to 2700 $cm^{-1}$, comprises phosphate units and Ca-O. In the 2250 to 1800 $cm^{-1}$ band region, the spectrum displays apatite vibrations. In the 2250 to 1800 $cm^{-1}$ band region, the spectrum displays apatite vibrations. In the spectral range of 3450-3300 $cm^{-1}$, the presence of OH, (OH)-, and F units is observed [9]-[11].

*C. SEM & EDS*

1. Results of SEM and EDS Studies on Sample SF1

Based on observations from SEM images and EDX analysis graph, the elements of sample SF-1 (Fig. 7) appear to be homogeneous but exhibit a relatively rough surface. According to petrographic and SEM studies, this sample may contain calcareous components along with oxidized portions (Fig. 7 (a)). On the other hand, the results obtained from the EDX analysis of sample SF-1 indicate significant concentrations of the elements P, Ca, and O, with minor elements Cl, F, and Na. Based on similar values of chlorine and fluorine, the sample can be designated as a fluor-chlorapatite (Fig. 7 (b)).

2. Results of SEM and EDS Studies on Sample SF2

Based on observations from SEM images and EDX analysis graph, the elements of sample SF-2 (Fig. 8) appear to be densely but exhibit a relatively rough surface. According to petrographic and SEM studies, this sample may contain calcareous components along with oxidized portions (Fig. 8 (a)) [11]. On the other hand, the results obtained from the EDX analysis of sample SF-2 indicate significant concentrations of the elements P, Ca, and O, with minor elements Cl, F, and Na. Based on high values of calcium, chlorine, the sample can be designated as a calcium chlorapatite (Fig. 8 (b)).

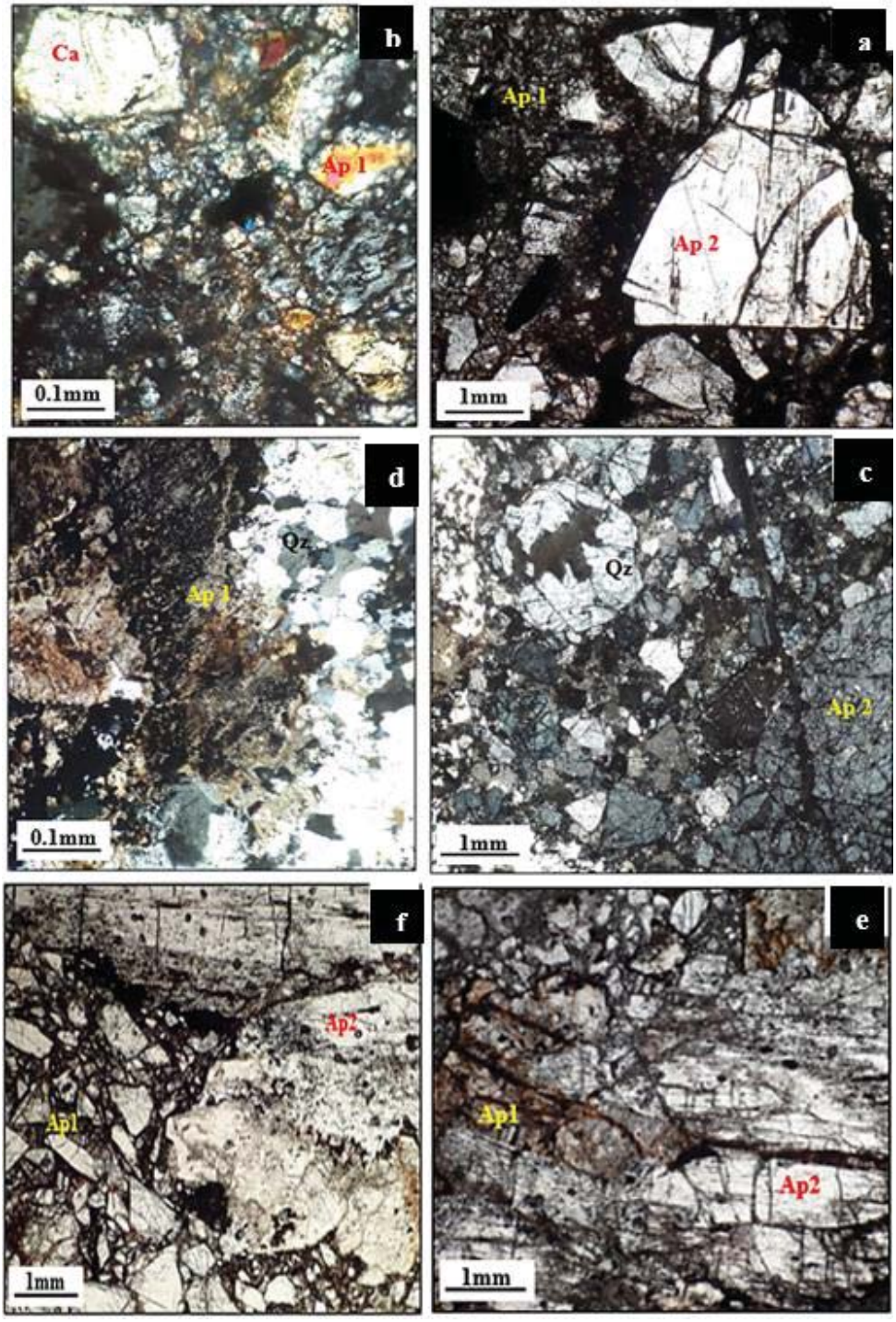


Fig. 3 Microscopic images of apatite crystals in thin section under two light modes, PPL (Plane-Polarized Light) and XPL (Cross-Polarized Light): (a) Large apatite crystals within a matrix of Opac (magnetite) minerals; (b) Apatite and calcite within a fractured and altered matrix (XPL); (c) Intergrowth of granitic quartz and second-generation apatite (XPL); (d) Replacement of granitic quartz by Anhedral microcrystals of apatite (in XPL); (e) Coarse-grained apatites of the second generation are observed within the vein section of the Esfordi mine, accompanied by first-generation apatites as replacements (PPL); (f) First and second generation apatites are found within a magnetite-rich matrix in the vein section of the Esfordi deposit (XPL)

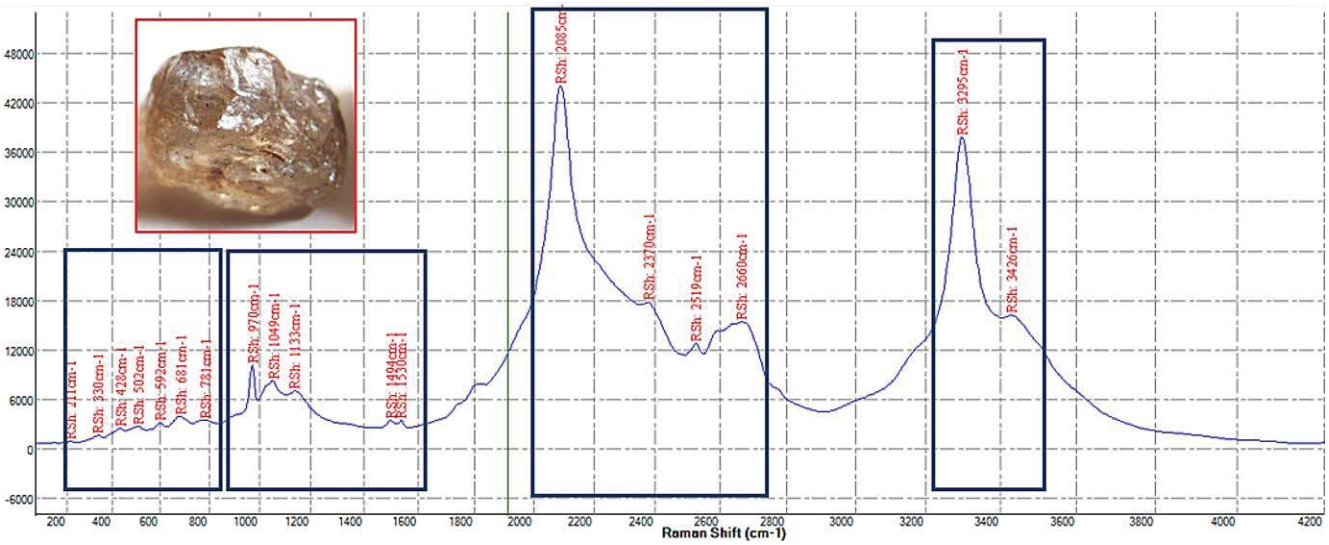


Fig. 4 Raman Spectrum of Sample SF-11 from the Esfordi Phosphate-Iron Mine

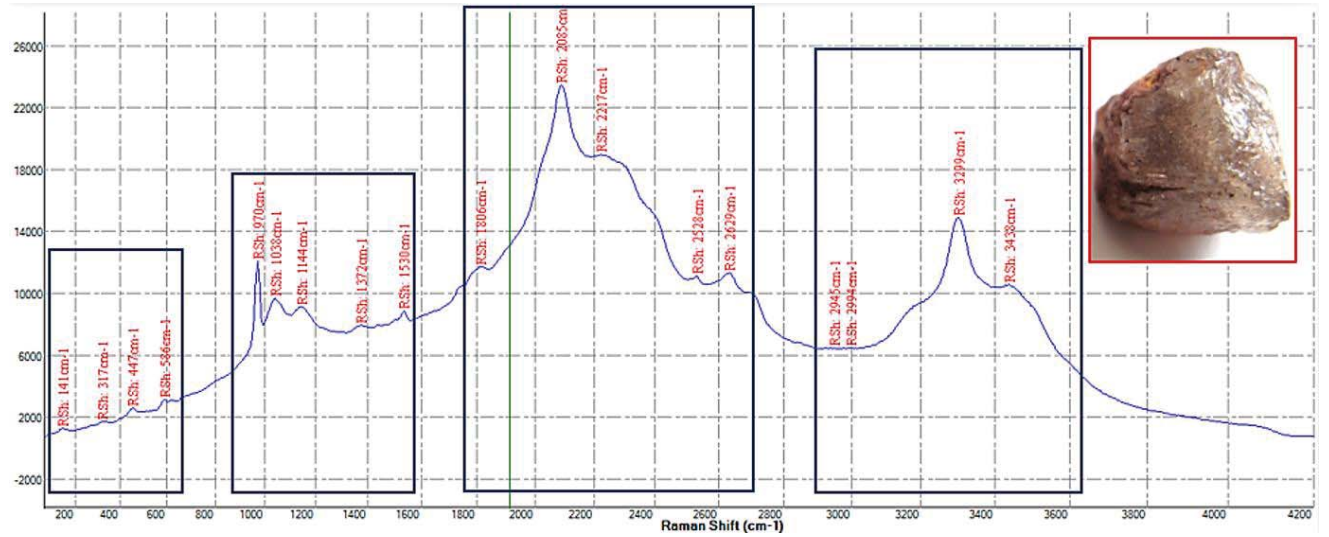


Fig. 5 Raman Spectrum of Sample SF-12 from the Esfordi Phosphate-Iron Mine

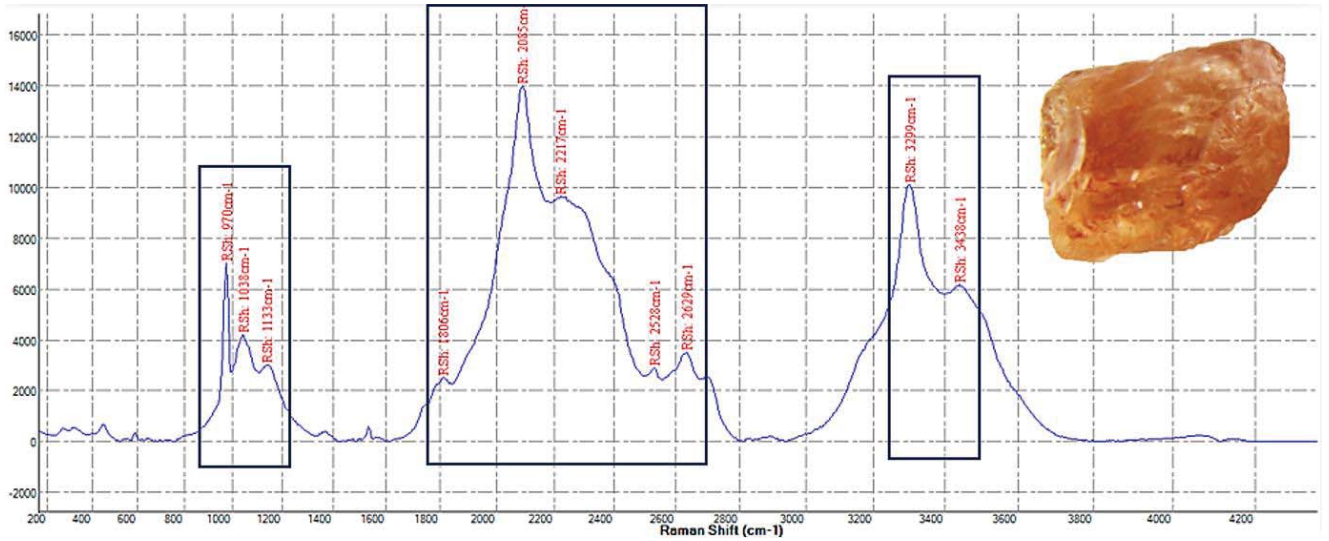


Fig. 6 Raman Spectrum of Sample SF-13 from the Esfordi Phosphate-Iron Mine

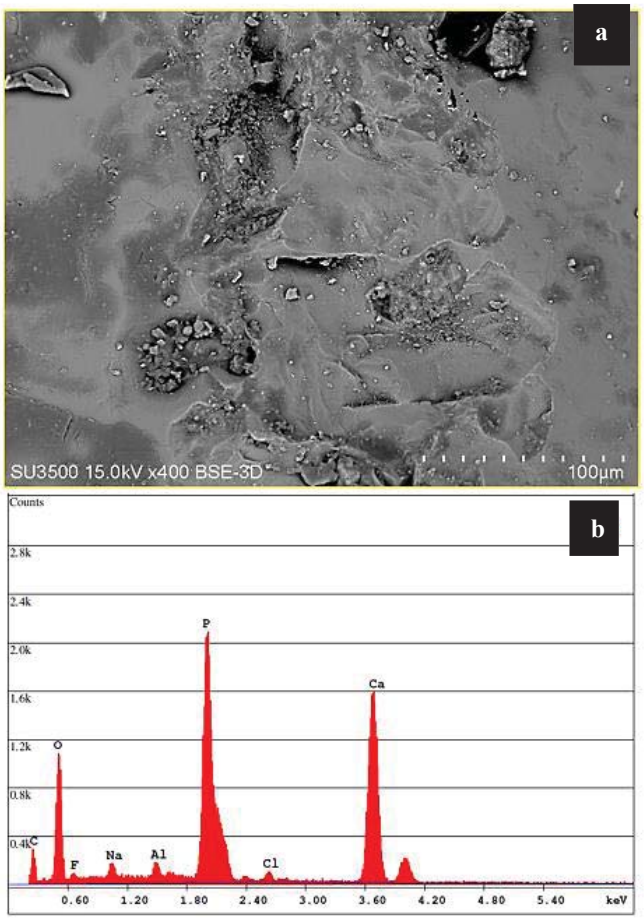


Fig. 7 (a) SEM image of SF-1 (apatite crystals from the Apatite-Iron deposit in Esfordi) with a magnification of 100 µm; (b) EDX analysis diagram of SF-1 showing major elements including P, Ca, and O and minor elements C, Cl, F, Al, Na

3. Results of SEM and EDS Studies on Sample SF3

Observations of SEM images and the EDX analysis graph of sample SF-3 (Fig. 9) indicate a chemically homogeneous and compact surface, which, based on petrographic and SEM studies, suggests that this sample contains calcareous components (Fig. 9 (a)) [11]. The additional results obtained from the EDX elemental analysis of sample SF-3 indicate abundant amounts of elements P, Ca, and C, with minor elements O, Cl, F, and Na present. In comparison to other samples, this sample exhibits significantly higher levels of carbon and lower levels of oxygen. Furthermore, in terms of abundance, the amount of calcium in this sample is much greater than in other samples. Based on the high concentrations of calcium and carbon, this sample can be designated as a pure apatite (see Fig. 9 (b)).

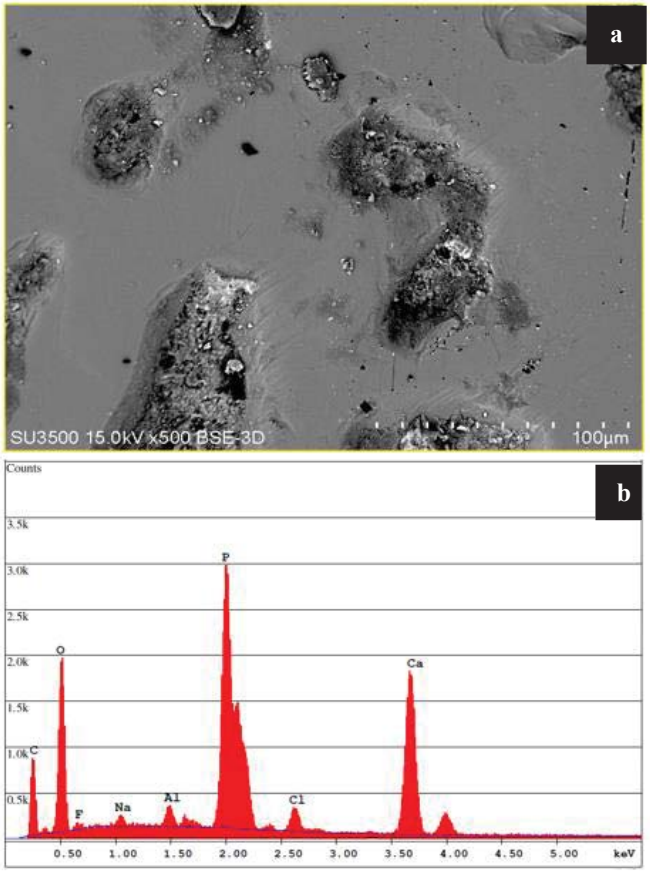


Fig. 8 (a) SEM image of SF-2 (apatite crystals from the Apatite-Iron deposit in Esfordi) with a magnification of 100 µm; (b) EDX analysis diagram of SF-2 showing major elements including P, Ca, and O and minor elements C, Cl, F, Al, Na

## V. Conclusion

1. The process of apatite formation in the volcanic rocks of the studied area can be associated with the intrusion of inner mass into the sedimentary and volcanic rocks of the region, followed by interaction with magmatic fluids.
2. Mineralogy of thin polished sections examined by transmitted and reflected light microscopes indicated the presence of pyrite and magnetite as the most abundant metallic minerals associated with apatite.
3. Calcium apatite and fluorapatite are the most important minerals studied in Esfordi.
4. Raman analysis graphs of the Esfordi samples shows very close coverage and coherence with each other, indicating a similarity in their crystalline network.
5. SEM analysis reveals that the studied samples from the Esfordi mining area exhibit a dense and coherent texture with smooth surfaces. Based on the elemental analysis results, the apatites in the Esfordi group are classified as calcic apatites because they are very rich in calcium and carbon but relatively poor and empty in terms of chlorine and fluorine content.

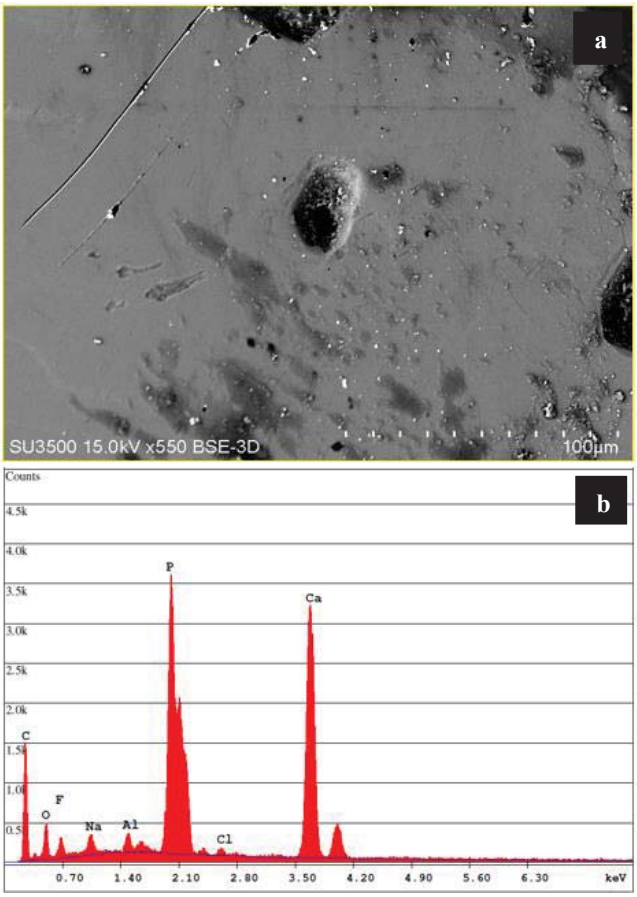


Fig. 9 (a) SEM image of SF-3 (apatite crystals from the Apatite-Iron deposit in Esfordi) with a magnification of 100 µm; (b) EDX analysis diagram of SF-3 showing major elements including P, Ca, and C and minor elements O, Cl, F, Al, Na

## REFERENCES

[1] Barati, M.B., Kadkhodaie, A., Soleimani, B., Saberi, F. and Asoude, P., 2023. Determination of reservoir parameters of the upper part of Dalan formation using NMR log and core in south pars oil field. *Journal of Petroleum Research*, *33*(1402-1), pp.73-83.

[2] Elyasi, A., Makarian, E. and Saberi, F., Fracture Gradient Prediction: Applicable to Safe Drilling and Underground Storage Operations.

[3] Elyasi, A., Makarian, E. and Saberi, F., Horizontal Stresses Prediction Using Sonic Transition Time Based on Convolutional Neural Network, https://www.searchanddiscovery.com/pdfz/documents/2023/42587makarian/ndx_makarian.pdf.html

[4] Larki, E., Jaffarbabaei, B., Soleimani, B., Elyasi, A., Saberi, F., Makarian, E., Shad Manaman, N. and Radwan, A.E., 2023. A new insight to access carbonate reservoir quality using quality factor and velocity deviation log. *Acta Geophysica*, pp.1-20.

[5] Hashemi, R., Saberi, F., Asoude, P. et al. 2024. Enhancing Reservoir Zonation through Triple Porosity System: A Case Study. *SPE J*. SPE-219491-PA (in press; posted 12 March 2024). https://doi.org/10.2118/219491-PA.

[6] Saberi, F and Hosseini-Barzi, M., New Achievement in the Effect of Clay Mineral on the Movement of Hydrocarbons in the Source Rock https://www.searchanddiscovery.com/documents/2023/51701saberi/ndx_saberi.pdf

[7] Saberi, F and Hosseini-Barzi, M., Investigating the Sediments of the Pabdeh Formation in Zagros Basin, Iran https://www.searchanddiscovery.com/documents/2023/51700saberi/ndx_saberi.pdf

[8] Rajabi, S., Ramazani, A., Hamidi, M. and Naji, T., 2015. Artemia salina as a model organism in toxicity assessment of nanoparticles. *DARU Journal of Pharmaceutical Sciences*, *23*, pp.1-6.

[9] Cejka, J., Sejkora, J., Macek, I., Malikova, R., Wang, L., Scholz, R., Xi, Y., Frost, R. L., (2015), Raman and infrared spectroscopic study of turquoise minerals, Spectrochimica Acta Part A: Molecular and Biomolecular Spectroscopy 149, 173–182.

[10] Saberi, F., Hosseini-Barzi, M. Effect of thermal maturation and organic matter content on oil shale fracturing (2024). https://doi.org/10.1007/s40789-024-00666-0

[11] Welton, J., SEM Petrology Atlas, (2003), The American Association of Petroleum Geologists, 240.